Traffic-Responsive Linked Ramp-Metering Control

Ioannis Papamichail and Markos Papageorgiou, *Fellow, IEEE*

***Abstract*—A new traffic-responsive ramp-metering strategy is presented that coordinates local ramp-metering actions, thus enabling the linked control of the inflow from two (or more) consecutive on-ramps to the freeway mainstream. The proposed linked ramp-metering scheme is simple and utterly reactive, i.e., based on readily available real-time measurements without any need for real-time model calculations or external disturbance prediction. The well-known feedback strategy, known as Asservissement LINéaire d'Entrée Autoroutière (ALINEA), is used at a local level. Simulation results are presented for a hypothetical freeway axis with two successive on-ramps. Some pitfalls and misapplications of the local ramp metering are also illustrated via appropriately designed simulation scenarios. The proposed linked strategy is demonstrated to outperform the uncoordinated local ramp metering and, thus, to increase the achievable control benefit over the no-control case. In fact, the new strategy is shown to reach the efficiency of sophisticated proactive optimal control schemes.**

***Index Terms*—ALINEA, coordinated ramp metering, HEuristic Ramp-metering coOrdination (HERO), linked control.**

I. Introduction

RAMP METERING, which is the most direct and efficient way to control freeway networks, aims at improving the traffic conditions by appropriately regulating the inflow from the on-ramps to the freeway mainstream. Traffic-responsive ramp-metering strategies, as opposed to fixed-time strategies, are based on real-time measurements from sensors installed in the freeway network and can be classified as local or coordinated.

Local ramp-metering strategies make use of measurements from the vicinity of a single ramp. Most prominent examples of the local ramp-metering strategies are the demand-capacity (DC) and the occupancy (OCC) strategies [1] and Asservissement Linéaire d'Entrée Autoroutière (ALINEA) strategy [2], [3] and its variations [4], [5]. The DC and the OCC are feedforward disturbance-rejection schemes that target the flow capacity in the merge area and are based on mainstream measurements of flow or occupancy, respectively, upstream from the ramp. It was found that the real flow capacity in a merge area may quite substantially vary from day to day, even under similar environmental conditions [6], [7]; thus, the DC and OCC strategies that target a prespecified flow capacity value may either overload or underutilize the freeway infrastructure. In contrast, the critical density (or occupancy) at which the capacity flow occurs was found to be more stable [8], [9].

On the other hand, the ALINEA strategy and its variations are feedback control schemes targeting a set point for the downstream occupancy or density (usually, the respective critical values) and utilizing the mainstream measurements of occupancy or density downstream of the ramp. It is probably because of this feedback structure and the targeting of the pretty stable critical occupancy (or density) that ALINEA was found to lead to significantly better performance than the DC and OCC strategies in several comparative field evaluations [3].

Coordinated ramp-metering strategies make use of the measurements from an entire region of the network to control all metered ramps included therein; they may be more efficient than the local ramp-metering strategies when there are multiple bottlenecks on the freeway or restricted ramp storage spaces. The coordinated ramp-metering approaches include sophisticated methods such as multivariable [10], [11] and optimal control strategies [12]–[17].

An extensive review of heuristic coordinated traffic-responsive ramp-metering algorithms was presented in [18]. A number of studies have compared the performances of some of these algorithms. Recently, the properties and the available comparison results for a number of heuristic coordinated strategies that have been implemented in the USA were summarized in [19], including the Zone and the Stratified Zone algorithms, the Bottleneck algorithm, and the Helper algorithm. The main drawbacks of these approaches are that they mostly apply low-accuracy feedforward schemes and that they target the (uncertain) flow capacity.

A new simple rule-based coordinated ramp-metering strategy, known as the HEuristic Ramp-metering coOrdination (HERO), is employed in this paper that includes ALINEA regulators at a local level. Although HERO can be applied as a coordinated strategy for arbitrarily sized and configured freeway networks [20], this paper focuses on its application as a linked-control approach for a couple of successive metered ramps. Linking of successive metered ramps is recommended whenever the available ramp storage space is limited, leading to excessive queue override and mainstream congestion. The presented simulation investigations demonstrate the increased efficiency of the linked control. In addition, the consideration of different control combinations may be useful in illustrating some misapplications of the local ramp-metering control that are frequently encountered in real installations of the local ramp-metering algorithms.

The rest of this paper is organized as follows. In Section II, the freeway-network traffic-flow model used for simulation purposes is briefly outlined. Section III presents the local ramp-metering strategies used, and their application to a

Manuscript received January 22, 2007; revised April 30, 2007, July 25, 2007, and July 31, 2007. This work was supported in part by the European Social Fund and National Resources—EPEAEK II (PYTHAGORAS II). The Associate Editor for this paper was H. Mahmassani.

The authors are with the Dynamic Systems and Simulation Laboratory, Department of Production Engineering and Management, Technical University of Crete, 73100 Chania, Greece (e-mail: ipapa@dssl.tuc.gr; markos@dssl.tuc.gr).

Digital Object Identifier 10.1109/TITS.2007.908724

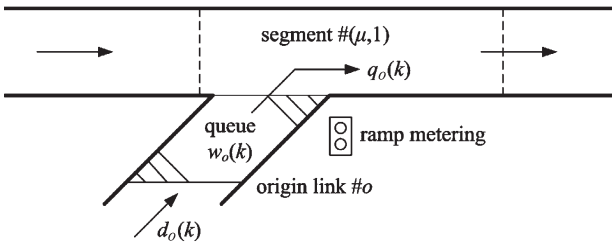

Fig. 1. Origin-link queue model.

hypothetical test freeway axis is investigated in Section IV. Section V introduces the new reactive linked-control approach, and the results from its application to the test freeway axis are presented in Section VI. The main conclusion is summarized in Section VII.

II. Traffic-Flow Modeling

The METANET freeway traffic-flow simulator [21] employing a macroscopic second-order traffic-flow model is used in this paper. The traffic-flow model was validated against real traffic data at several instances [22], [23] and was found to reproduce the real traffic conditions with remarkable accuracy. The model parameter values used in this paper are taken from a previous model calibration for a real freeway [23]. The freeway network is represented by a directed graph whereby the links of the graph represent freeway stretches. Each freeway stretch has uniform characteristics, i.e., no on-/off-ramps and no major changes in geometry. The nodes of the graph are placed at locations where a major change in road geometry occurs, as well as at junctions and at on- and off-ramps.

The time and space arguments are discretized. The discrete time step is denoted by T (typically, $T \simeq 10$ s). A freeway link m is divided into N_m segments of equal length L_m (typically, $L_m \simeq 500$ m) such that the numerical stability condition $L_m \geq T \cdot \nu_{f,m}$ holds, where $\nu_{f,m}$ is the free speed of link m. Each segment i of link m at discrete time $t = kT$, $k = 0, \ldots, K$, where K is the time horizon, is macroscopically characterized via the following variables: The traffic density $\rho_{m,i}(k)$ (in veh/km/lane) is the number of vehicles in segment i of link m at time $t = kT$ divided by L_m and by the number of lanes, the mean speed $\nu_{m,i}(k)$ (in km/h) is the mean speed of the vehicles included in segment i of link m at time $t = kT$, and the traffic volume or flow $q_{m,i}(k)$ (in veh/h) is the number of vehicles leaving segment i of link m during the time period $[kT, (k+1)T]$, which is divided by T.

The evolution of traffic state in each segment is described by the use of two interconnected state equations for the traffic density and the mean speed, respectively. Roughly speaking, the flow increases with an increasing density until a density critical value is reached, at which the flow becomes maximum. After this critical density, congestion sets on, and the flow decreases, reaching virtually zero at a jam density value.

For origin links, i.e., links that receive traffic demand d_o and forward it into the freeway network, a simple queue model is used (Fig. 1). The outflow q_o of the origin link o not only depends on the arriving demand d_o and the ramp queue w_o (if any) but also on the traffic conditions of the corresponding mainstream segment (μ, 1) and the existence of the ramp-metering control measures. More specifically, the ramp-outflow capacity is linearly reduced with an increasing density $\rho_{\mu,1}$ beyond the critical density value, and thus, a ramp queue may appear even without ramp metering due to the mainstream congestion. If ramp metering is applied, then the outflow that is allowed to leave the origin o during period k is determined by the control law used. The evolution of the origin queue w_o is described by an additional state equation (conservation of vehicles).

Note that the freeway flow $q_{\mu,1}$ in merge segments is maximized if the corresponding density takes values around a critical density $\rho_{cr,\mu}$. Due to the complex nonlinear and dynamic nature of the macroscopic model, the critical density (at which the highest flows are observed) may be determined via simulation, i.e., by noticing the density value at which the mainstream flow is highest.

III. Local Ramp-Metering Strategies

For each on-ramp o with a merging segment (μ, 1) (Fig. 1), a local regulator with control sample time T_c, which is a multiple of the model sample time T, i.e., $T_\mathrm{c} = z_\mathrm{c}T$, $z_\mathrm{c} \in \mathbb{N}$ (e.g., $T_\mathrm{c} = 3T = 30$ s), can be applied as a stand-alone strategy without any kind of coordination. Let $k_\mathrm{c} = \mathrm{int}[k/z_\mathrm{c}]$. For simplicity of notation, all model variables used in the following as emulated measurements by the regulators are assigned with a discrete-time index k_c; for example, when the model merge-area density $\rho_{\mu,1}(k)$ is picked every T_c for regulator usage, it is denoted as $\rho_o(k_\mathrm{c})$, where $\rho_o(k_\mathrm{c}) = \rho_{\mu,1}(k_\mathrm{c}z_\mathrm{c})$. Then, the discrete-time I-type regulator ALINEA with a set point $\tilde{\rho}_o$ reads

$$q_o^r(k_\mathrm{c}) = q_o^r(k_\mathrm{c} - 1) + K_\mathrm{I}\left[\tilde{\rho}_o - \rho_o(k_\mathrm{c})\right] \tag{1}$$

where $K_\mathrm{I} > 0$ is the feedback gain factor, $\rho_o(k_\mathrm{c})$ is the measurement of the traffic density from the merging segment, and $q_o^r(k_\mathrm{c})$ is the outflow ordered by the regulator. Typically, the set point used is set equal to the critical density of the corresponding area in order to maximize the downstream freeway flow.

In some cases, congestion is not created because of merging, but it appears first at a bottleneck situated further downstream that has lower capacity than the merging area. Such a bottleneck may be due to a lane drop, a strong slope, a curvature, or an uncontrolled downstream ramp. Whatever is the reason, the created congestion propagates upstream and reaches the merge area of the controlled ramp. In this case, it is imperative to control the ramp flow using the measurements (and set point) from the downstream bottleneck rather than from the merge area. However, this may lead to ALINEA control oscillations, as it was pointed out in [24]. For this case, a Proportional-Integral (PI) extension of ALINEA has been suggested [24] that reads

$$\begin{aligned} q_o^r(k_\mathrm{c}) = q_o^r(k_\mathrm{c} - 1) &- K_\mathrm{P}\left[\rho_o(k_\mathrm{c}) - \rho_o(k_\mathrm{c} - 1)\right] \\ &+ K_\mathrm{I}\left[\tilde{\rho}_o - \rho_o(k_\mathrm{c})\right] \end{aligned} \tag{2}$$

where $K_\mathrm{P} > 0$ is the gain factor for the proportional term added, and $\rho_o(k_\mathrm{c})$ is now the measurement of the traffic density from the downstream bottleneck.

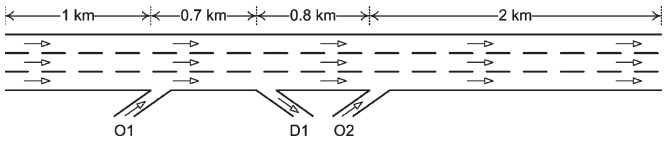

Fig. 2. Test three-lane freeway axis with two on-ramps.

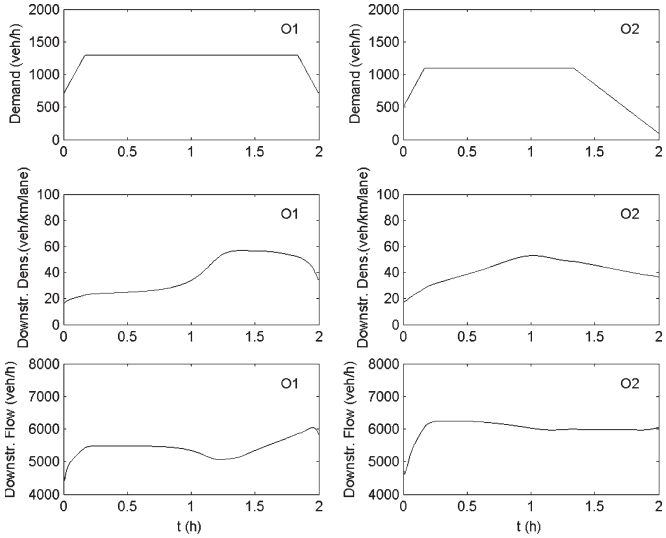

Fig. 3. No-control case (scenario 1).

Creation of long ramp queues can be avoided with the application of a queue-control policy [4] in conjunction with any local ramp-metering strategy (1) or (2). The queue-control law takes the form

$$q_o^w(k_c) = -\frac{1}{T_c}\left[w_{\max,o} - w_o(k_c)\right] + d_o(k_c - 1) \qquad (3)$$

where $q_o^w(k_c)$ is the ramp outflow ordered, $w_{\max,o}$ is the maximum admissible number of vehicles in the queue of the on-ramp o, and d_o is the arriving ramp demand. The final on-ramp outflow is then

$$q_o(k_c) = \max\left\{q_o^r(k_c), q_o^w(k_c)\right\} \qquad (4)$$

where $q_o^r(k_c)$ may be calculated by either (1) or (2).

The calculated $q_o(k_c)$ is bounded by the ramp's flow capacity $q_{\max,o}$ and the minimum admissible ramp flow $q_{\min,o}$. In order to avoid the well-known wind-up phenomenon of the I-type regulators (i.e., continued accumulation of the regulation error when control constraints are active), the term $q_o^r(k_c - 1)$ used in both (1) and (2) is also accordingly bounded.

IV. Application of Local Strategies

A. Test Freeway Axis

For the purposes of this paper, a long three-lane freeway axis of 4.5 km, which is shown in Fig. 2, is considered. There are two on-ramps (O1 and O2) on this freeway and one off-ramp (D1) in between. The trapezoidal demand profiles, which are shown in (both upper diagrams of) Fig. 3, are used for the two on-ramps, whereas a constant demand of 4200 veh/h is considered for the mainstream flow. The exit rate, i.e., the percentage of the mainstream flow that leaves the freeway, at the off-ramp D1 is set to 5%, and the model time step used in the METANET simulator is $T = 10$ s. A number of different scenarios, which are presented in Table I, are examined in the following, each for a time horizon of 2 h. The application of the known local-control strategies (in various combinations) will be presented first in order to motivate the introduction of the linked control later on.

B. No-Control Case

When no control measures are applied (scenario 1), the resulting density and flow profiles for both merge areas are shown in Fig. 3. Mainstream congestion appears after 30 min in the merge area of the O2 on-ramp due to the higher flows that arrive there; this leads to a visible gradual mainstream-flow decrease (capacity drop). The created congestion travels upstream and reaches the merge area of the O1 on-ramp at around $t = 1$ h, also leading to a visible flow decrease. In this scenario, no queues are formed at the on-ramps.

The resulting Total Time Spent (TTS) (in veh · h) of all vehicles in the network (which is calculated to include the possible waiting time experienced in the ramp queues) is equal to 983 veh · h. The TTS was calculated over the 2 h of simulation shown in the figures plus a cool-down period of 5 min with zero inflows, which was introduced in order to have equal traffic conditions on the stretch (empty network) at the end of the simulation and, hence, comparable TTS values for all investigated scenarios. On the other hand, as the traffic conditions in all investigated scenarios of Table I are virtually identical over the first 30 min of the simulation (warm-up period before congestion creation), the TTS is also calculated, excluding the first 30 min of the simulation (TTS′). Moreover, the Total Waiting Time (TWT) (the number of vehicles times the number of hours) at the on-ramps is calculated for comparison among the control scenarios. Note that the TWT is a part of the TTS and that TWT′ = TWT since no ramp queue appears in any control scenario during the first 30 min of the simulation. For the no-control case (scenario 1), the TTS′ is equal to 817 veh · h, whereas the TWT is equal to zero (no ramp queues).

C. Application of ALINEA and Its PI Extension

In order to apply the ALINEA regulator or its PI extension, the critical densities are needed for the two merge areas. With simulation checking, the critical density for the merge area downstream of O1 is found to be equal to 33 veh/km/lane, whereas the critical density for the merge area downstream of O2 is equal to 38 veh/km/lane. Whenever ALINEA is used, the gain factor K_I is set equal to 32 km · lane/h. Whenever the PI extension of ALINEA is used, the gain factors K_P and K_I are set to 100 and 4 km · lane/h, respectively, according to the findings in [24]. The control sample time T_c is equal to 30 s. The minimum admissible ramp flow for each on-ramp is set to 200 veh/h, whereas their flow capacity is set to 1600 veh/h.

In the second scenario studied, ALINEA is applied to O2 without queue constraints ($w_{\max,o} = +\infty$), whereas no-control measure is applied to O1. Then, the mainstream outflow is indeed maximized, and hence, a significant amelioration of

TABLE I
SCENARIOS STUDIED AND RESULTS ACHIEVED FOR THE TRAPEZOIDAL DEMANDS

scenario	strategy on O1	meas. point	max queue at O1 (veh)	strategy on O2	meas. point	max queue at O2 (veh)	TWT (veh·h)	TTS (veh·h)	TTS' (veh·h)	% decr. on TTS'
1	no-control	-	-	no-control	-	-	0	983	817	0.0
2	no-control	-	-	ALINEA	O2	$+\infty$	104	868	702	14.1
3	no-control	-	-	ALINEA	O2	50	64	918	752	8.0
4	ALINEA	O1	$+\infty$	no-control	-	-	86	953	787	3.7
5	ALINEA	O1	50	no-control	-	-	46	975	809	1.0
6	ALINEA	O2	$+\infty$	no-control	-	-	146	893	727	11.0
7	ALINEA	O2	50	no-control	-	-	67	921	755	7.6
8	PI-ALINEA	O2	$+\infty$	no-control	-	-	114	869	703	14.0
9	PI-ALINEA	O2	50	no-control	-	-	67	915	749	8.3
10	ALINEA	O1	50	ALINEA	O2	50	78	908	742	9.2
11	AMOC	-	50	AMOC	-	50	94	871	705	13.7
12	LC	O1	50	LC(30%-15%)	O2	50	98	874	708	13.3
13	LC	O1	50	LC(80%-40%)	O2	50	98	874	708	13.3
14	ALINEA	O1	70	ALINEA	O2	30	79	926	760	7.0
15	AMOC	-	70	AMOC	-	30	94	872	706	13.6
16	LC	O1	70	LC(30%-15%)	O2	30	97	878	712	12.9

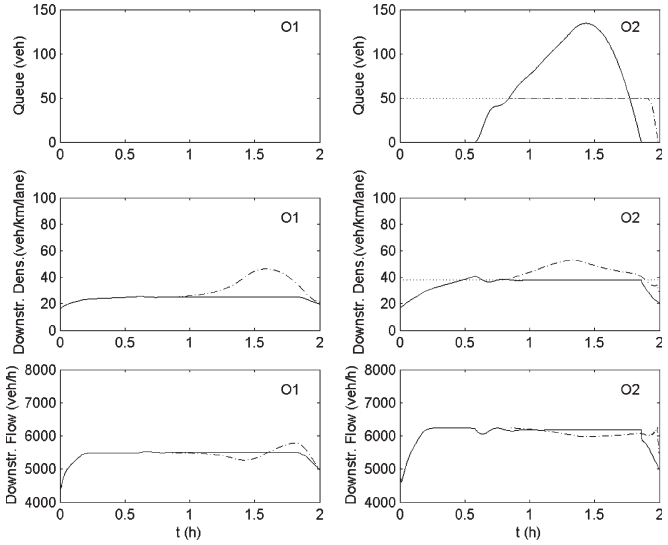

Fig. 4. ALINEA at O2 without queue constraints (scenario 2 with solid lines) and with an admissible queue equal to 50 veh (scenario 3 with dash-dotted lines).

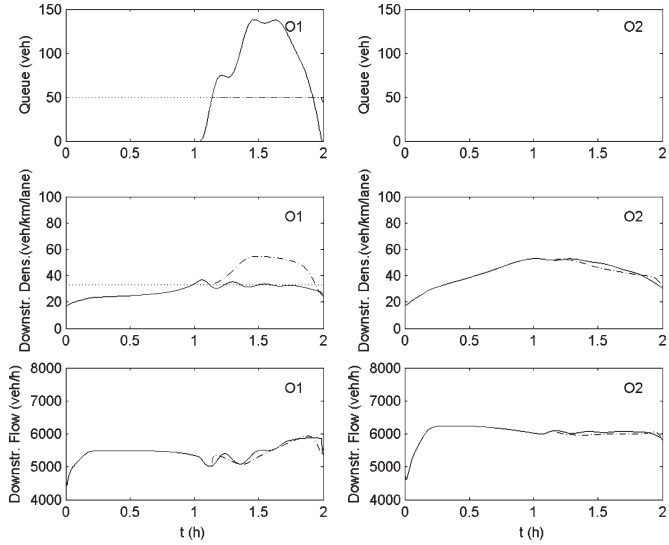

Fig. 5. ALINEA at O1 without queue constraints (scenario 4 with solid lines) and with an admissible queue equal to 50 veh (scenario 5 with dash-dotted lines).

the traffic conditions is achieved. The TTS′ is reduced to 702 veh · h (Table I), which is a 14.1% improvement compared with the no-control case, whereas the TWT is equal to 104 veh · h. The related ramp-queue, density, and flow profiles for both merge areas are shown in Fig. 4 (solid lines). The dotted curves appearing in all figures correspond to the utilized set points. Note that there is no queue in the uncontrolled O1 on-ramp, but the achieved improvement comes at the expense of a long queue formed at the O2 on-ramp. This queue is likely to cause traffic problems in the adjacent street junction upstream from the ramp, affecting the attached urban network. Additionally, this approach is strongly unfair toward the drivers served by the O2 on-ramp.

If the queue-control policy is active with a maximum admissible ramp queue equal to 50 veh (scenario 3), ALINEA is seen to become less efficient because the congestion cannot be avoided due to the limited ramp storage. The resulting TTS′ is equal to 752 veh · h, which is an 8.0% improvement compared with the no-control case, whereas the TWT is equal to 64 veh · h. The related ramp-queue, density, and flow profiles for both merge areas are shown in Fig. 4 (dash-dotted lines). It may be seen that the queue at the O2 on-ramp now reaches its maximum admissible value and is maintained there by the queue control (3). As a consequence, the density in the merge area of O2 departs from its set point, i.e., freeway congestion is created that travels upstream and leads to correspondingly reduced mainstream throughput.

In the next six scenarios, the no-control measure is applied to O2. In scenario 4, ALINEA is applied at O1 without ramp queue constraints, and the related ramp-queue, density, and flow profiles for both merge areas are shown in Fig. 5 (solid lines). As in scenario 1, the mainstream congestion first appears in the merge area of the O2 on-ramp due to the higher flows that arrive there. The created congestion travels upstream and reaches the merge area of the O1 on-ramp, triggering the ALINEA

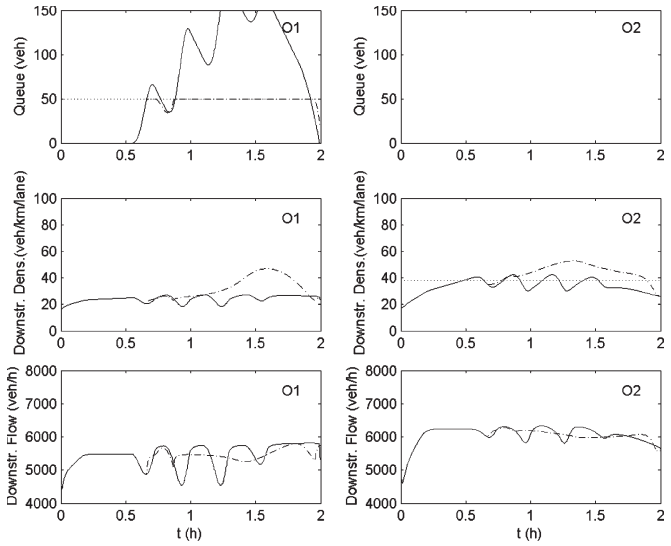

Fig. 6. ALINEA at O1 with measurements from O2 without queue constraints (scenario 6 with solid lines) and with an admissible queue equal to 50 veh (scenario 7 with dash-dotted lines).

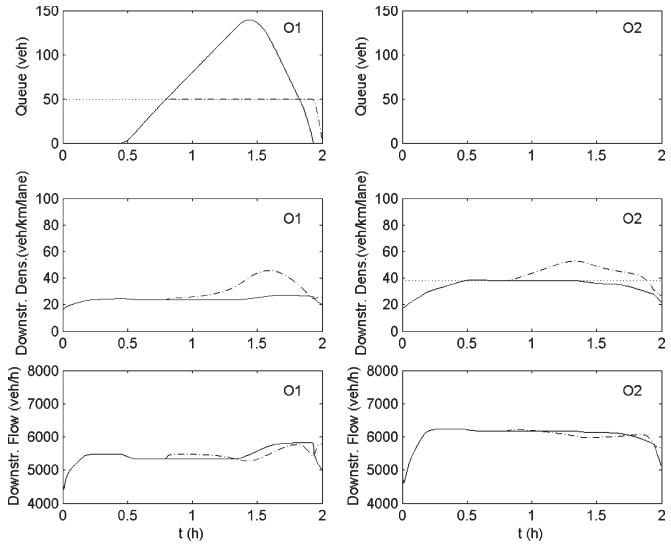

Fig. 7. PI-ALINEA at O1 with measurements from O2 without queue constraints (scenario 8 with solid lines) and with an admissible queue equal to 50 veh (scenario 9 with dash-dotted lines).

activation at O1. ALINEA attempts to maintain the density in the merge area of O1 around its critical value, but this leads to an oscillation of the density (and, eventually, of the flow) in the merge area due to the fact that the bottleneck is situated further downstream, in the merge area of O1. More precisely, restricting the O1 ramp flow via ALINEA reduces the targeted merge-area density, but this merely moves the congestion tail a little further downstream without dissolving it because the congestion head is still maintained in the O2 merge area. In other words, the observed oscillations correspond to the locally limited upstream/downstream movements of the congestion tail, but, in fact, the mainstream congestion is never dissolved. Thus, the mainstream outflow remains reduced (capacity drop) due to the congestion, and the resulting TTS$'$ is equal to 787 veh $\cdot$ h, which is just a 3.7% improvement, compared with the no-control case, whereas the TWT is equal to 86 veh $\cdot$ h. If the queue-control policy is activated at O1 via a maximum admissible ramp queue equal to 50 veh (scenario 5), ALINEA becomes even less efficient, with a TTS$'$ equal to 809 veh $\cdot$ h, which is just a negligible 1.0% improvement compared with the no-control case, whereas the TWT is equal to 46 veh $\cdot$ h. The related ramp-queue, density, and flow profiles for both merge areas are shown in Fig. 5 (dash-dotted lines). Note that this scenario corresponds to the majority of current field installations of ramp metering which fail to achieve substantial benefits due to congestion shock waves arriving from downstream (and lack of coordination among the ramps).

In scenario 6, ALINEA is applied once more at O1 without the queue constraints. The difference from scenario 4 is that this time, the measurements of density for the ALINEA operation at O1 are taken from the merge area of O2 (further downstream bottleneck). The related ramp-queue, density, and flow profiles for both merge areas are shown in Fig. 6 (solid lines). Although the resulting TTS$'$ is equal to 727 veh $\cdot$ h, which is an 11.0% improvement compared with the no-control case (at the expense of a long queue formed at the O1 on-ramp; TWT is equal to 146 veh $\cdot$ h), strong oscillations with high amplitudes are seen for all variable trajectories, particularly the flow trajectory. These oscillations appear even for smaller values of the gain parameter used within ALINEA and are due to the inappropriate ALINEA structure in the case of a further downstream bottleneck that was already demonstrated in [24]. If the queue-control policy is active with a maximum admissible ramp queue equal to 50 veh (scenario 7), the resulting TTS$'$ is equal to 755 veh $\cdot$ h, which is a 7.6% improvement compared with the no-control case, whereas the TWT is equal to 67 veh $\cdot$ h. The related ramp-queue, density, and flow profiles for both merge areas are shown in Fig. 6 (dash-dotted lines).

In scenario 8, the PI extension of ALINEA is applied at O1 with the measurement collected at the merge area of O2 and without the queue constraints. The related ramp-queue, density, and flow profiles for both merge areas shown in Fig. 7 (solid lines) demonstrate a proper control action without oscillation. As in scenario 2, there is a significant amelioration of the traffic conditions, and the resulting TTS$'$ is reduced to 703 veh $\cdot$ h, which is a 14.0% improvement compared with the no-control case. However, in order to achieve this improvement, a long queue is formed at the O1 on-ramp; the TWT is equal to 114 veh $\cdot$ h. If the queue-control policy is active with a maximum admissible ramp queue equal to 50 veh (scenario 9), the control actions are still appropriate but are less efficient due to the limited ramp queue. The resulting TTS$'$ becomes 749 veh $\cdot$ h, which is an 8.3% improvement compared with the no-control case, whereas the TWT is equal to 67 veh $\cdot$ h. The related ramp-queue, density, and flow profiles for both merge areas are shown in Fig. 7 (dash-dotted lines). The queue at O1 is seen to reach its maximum admissible value, after which the freeway congestion is created in the merge area of O2 that travels upstream.

In scenario 10, ALINEA is applied at both O1 and O2. The queue-control policy is active with maximum admissible ramp queues equal to 50 veh. The related ramp-queue, density, and flow profiles for both merge areas are shown in Fig. 8. The queue at O2 reaches its maximum admissible

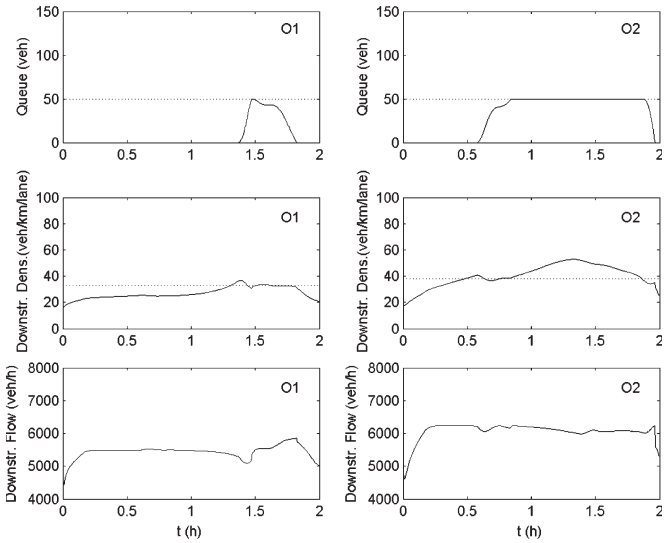

Fig. 8. ALINEA at O1 and O2 with admissible queues equal to 50 veh (scenario 10).

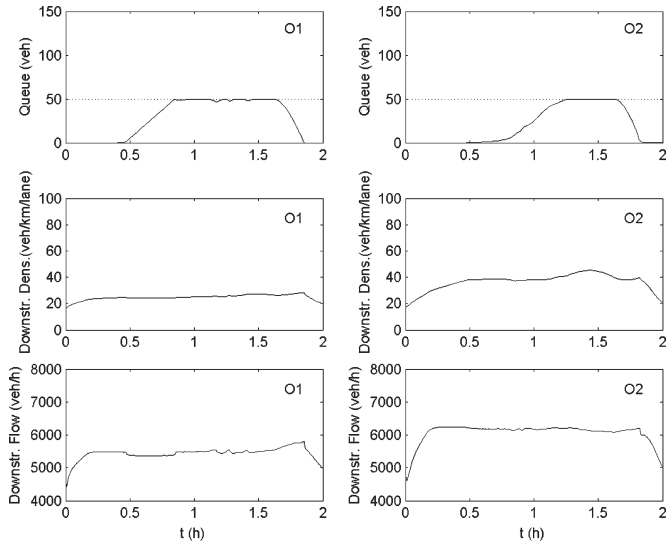

Fig. 9. Optimal open-loop solution (AMOC) with admissible queues equal to 50 veh (scenario 11).

value, and the freeway congestion is created that travels upstream and activates ALINEA at O1, leading to the spread of ramp queues, in reaction to the congestion that has formed. Note that, once the congestion created in the O2 merge area has reached the O1 merge area, the situation becomes identical to the inadequate control scenario 5, as discussed earlier. Fortunately, in this scenario, the congestion reaches the O1 merge area quite late, and hence, the TTS′ is equal to 742 veh · h, which is a 9.2% improvement compared with the no-control case, whereas the TWT is equal to 78 veh · h. Up to now, application of the uncoordinated ALINEA strategy to both on-ramps is the most efficient control structure when the storage space at each on-ramp is limited. Nevertheless, the mainstream congestion cannot be fully and adequately addressed.

D. Summarized Conclusions

The reported results illustrate the following general statements.

1) While many upstream ramps may contribute to the increase of mainstream flow in the uncontrolled case (scenario 1), a merge congestion eventually appears at one downstream ramp.
2) If local ramp metering with unlimited (or sufficiently high) ramp storage could be applied to the last downstream ramp (where the congestion appears—scenario 2), control efficiency would be very high, albeit at the expense of unfairly long waiting times at that particular ramp.
3) It makes little sense to apply the local ramp metering to ramps where mainstream congestion is imported from downstream (scenarios 4 and 5). What is needed in this case is a downstream bottleneck control via PI-ALINEA (scenarios 8 and 9) or a linked control.

In view of these statements, the linked control should attempt to approach the efficiency of scenario 2 (unlimited storage space at the most downstream ramp); more specifically, as the unlimited ramp storage space is not available, the available upstream ramp storage space should be exploited early enough to delay, or even avoid, the downstream congestion. This basic idea is implemented in the linked-control strategy to be presented in the next section.

V. Linked Control

The determination of the optimal on-ramp outflows that minimize a natural objective like the TTS value under limited ramp storage space can be achieved through the formulation and solution of a related optimal control problem, as implemented in the generic Advanced Motorway Optimal Control (AMOC) tool [15], [16]. This optimal open-loop solution, which is derived under the assumption of a perfect model and a perfect information with respect to the future disturbances (i.e., demand and exit-rate profiles), results in a TTS′ value equal to 705 veh · h, which is a 13.7% improvement compared with the no-control case, whereas the TWT is equal to 94 veh · h. The related ramp-queue, density, and flow profiles for both merge areas are shown in Fig. 9. Interestingly, but not surprisingly, the optimal solution maintains the density and flow at the O2 merge area, as long as possible, close to the critical and capacity values, respectively, to maximize the freeway exit flow (which leads to the minimization of TTS). To achieve this, similar ramp queues are simultaneously created in both ramps early in the simulation in anticipation of the future high demand. A slight congestion appearing at around $t = 1.3$ h is unavoidable in view of the high involved demands and limited ramp queues. Of course, this solution (scenario 11) serves as an "upper bound" for the achievable efficiency of any ramp-metering strategy as it relies on ideal conditions.

Note that the efficiency of AMOC may moderately but increasingly deteriorate with increasing disturbance-prediction errors or in case of model-versus-reality mismatch. Moreover, AMOC is a rather complex code incorporating a full macroscopic mathematical model of the traffic-flow process,

as well as a numerical solution algorithm for the addressed optimal control problem; code complexity, relatively intensive computations, and "black box" character of the optimization procedure may be perceived as obstacles for ready and broad application of the method.

In view of this discussion, it would be desirable to have a ramp-metering strategy that possesses the following features.

1) It should coordinate the local ramp-metering actions in a suitable way to avoid the pitfalls of the uncoordinated ALINEA application.
2) It should be simple and transparent, e.g., rule-based.
3) It should be reactive so that no external disturbance prediction is needed.
4) It should approach the efficiency of the sophisticated optimal control schemes.
5) It should be generic (i.e., directly applicable to any freeway network), without a need for cumbersome parameter calibration or fine-tuning.

A linked-control strategy possessing all the mentioned features was indeed developed and extensively tested via simulation. The new strategy exchanges data with and coordinates local ALINEAs (1), which are operated with a set point equal to the critical density of the corresponding merge area. Coordination is materialized via occasional setting of a minimum ramp queue length $w_{\min,o}$ that should be created and maintained at the upstream on-ramp O1. To this end, a slight extension of the local-control logic was introduced to enable the creation of the minimum queue length $w_{\min,o}$ ordered by the linked-control strategy. More specifically, the following additional control law is included in the local control actions for the on-ramp O1:

$$q_o^{\mathrm{LC}}(k_{\mathrm{c}}) = -K_{\mathrm{w}}\left[w_{\min,o} - w_o(k_{\mathrm{c}})\right] + d_o(k_{\mathrm{c}}-1) \qquad (5)$$

where K_{w} is a control parameter that may be set equal to $1/T_{\mathrm{c}}$ [as in (3)] for dead-beat queue control or lower for smoother control action. Equation (4) is then replaced as follows for the calculation of the final on-ramp outflow:

$$q_o(k_{\mathrm{c}}) = \max\left\{\min\left\{q_o^r(k_{\mathrm{c}}), q_o^{\mathrm{LC}}(k_{\mathrm{c}})\right\}, q_o^w(k_{\mathrm{c}})\right\}. \qquad (6)$$

The working principle of the new linked-control strategy is detailed as follows.

1) Every T_{c}, the current ramp queue lengths and the mainstream densities are received from the local controls; based on these data (no prediction), possible coordination actions are decided.
2) Whenever the relative ramp queue $w_o/w_{\max,o}$ of the downstream on-ramp (master) exceeds a certain activation threshold while the merge density is close to (or higher than) the critical density (i.e., the set-point), the linked-control strategy is activated. The reason for this activation is that the corresponding local ALINEA (1) is obviously active, and the formed queue may soon reach its maximum admissible value, leading to queue control and, eventually, mainstream congestion.
3) The activation of the linked-control strategy aims at enlarging the available storage space in order to avoid the congestion. To this end, a minimum queue $w_{\min,o}$ is ordered at the next upstream controllable on-ramp (slave) such that the relative queues of both ramps are close to each other, i.e., the relative free storage space in both ramps are equal. This coordination action holds the traffic back in the slave ramp (to reach the ordered $w_{\min,o}$), thus releasing the pressure from the master ramp. At the same time, the risk of overspilling of any ramp is minimized.
4) As the demand increases, the queue of the master ramp may continue to increase (albeit at a lower pace due to the coordination); in any case, the linked-control strategy is updating the $w_{\min,o}$ of the slave ramp each T_{c} such that the relative queues at both ramps are maintained close to each other.
5) When the relative queue of the master ramp falls below a deactivation threshold or its mainstream density becomes clearly undercritical, the coordination is then deactivated.

A flowchart of this algorithm is shown in Fig. 10. Two new variables (O1_TYPE and O2_TYPE) are used to specify the role of each ramp in the coordination scheme. These variables are initially given the value NOT_USED. This coordination scheme may readily be extended to apply to more than two consecutive ramps. In fact, the coordinated strategy can be further generalized to apply to the arbitrarily sized or configured freeway networks in the form of the HERO strategy [20].

VI. Application of Linked Control

As mentioned earlier, ALINEA is applied to both O1 and O2 as a basis for the linked control. The queue-control policy is active with maximum admissible ramp queue equal to 50 veh for each ramp, whereas possible minimum queues ordered by the master are handled based on (5) and (6). The activation threshold for the linked control is set to 30%, whereas the deactivation threshold is set to 15%, while the control parameter K_{w} is set equal to $0.1/T_{\mathrm{c}}$ (scenario 12). The resulting TTS$'$ is equal to 708 veh $\cdot$ h, which is a 13.3% improvement compared with the no-control case and just a 0.4% worsening compared with the optimum open-loop solution achieved by AMOC, and, as previously mentioned, it serves as an "upper bound" for the achievable efficiency. The TWT is equal to 98 veh $\cdot$ h. The related ramp-queue, density, and flow profiles for both merge areas are shown in Fig. 11 (solid lines). The linked control is seen to gradually increase both ramp queues quasi-simultaneously and to maintain the density in the O2 merge area close to its set point (critical density) at which the capacity flow occurs. When both ramp queues reach (again, quasi-simultaneously) their maximum admissible values, the respective queue controls (3) are activated, and an unavoidable slight congestion is created. This behavior is quite similar to the one exhibited by the optimal control (Fig. 9) and indeed results in an only slightly higher TTS value.

In order to investigate the sensitivity of the obtained coordination results with respect to the utilized activation and deactivation thresholds, simulations were conducted also for

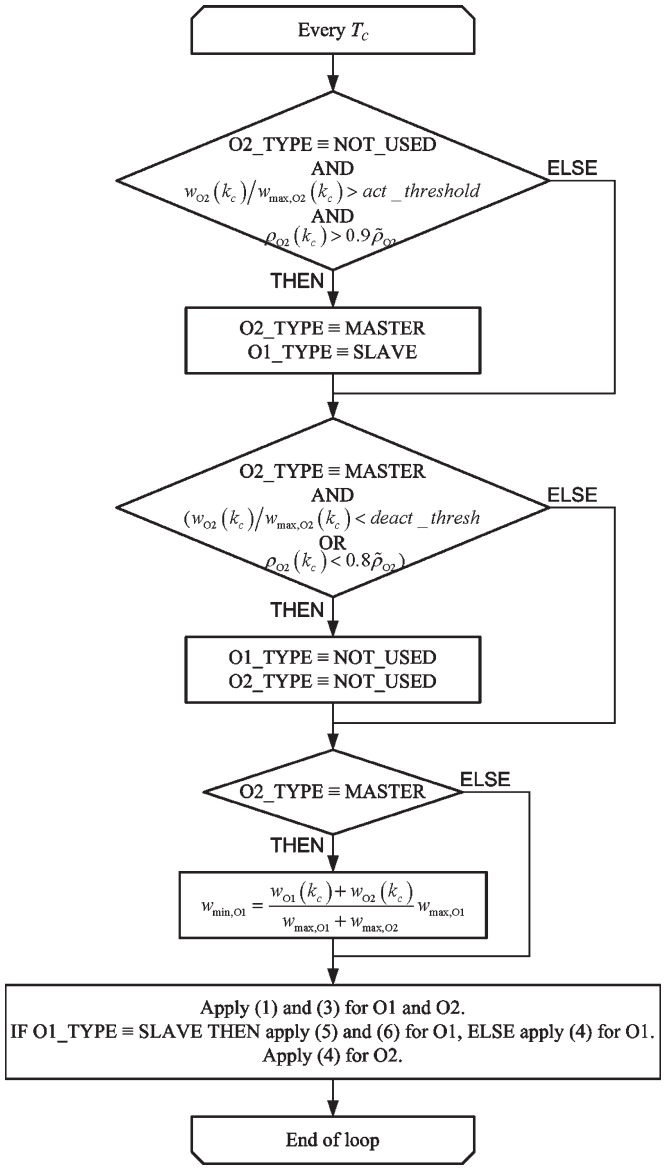

Fig. 10. Flowchart of the linked-control strategy.

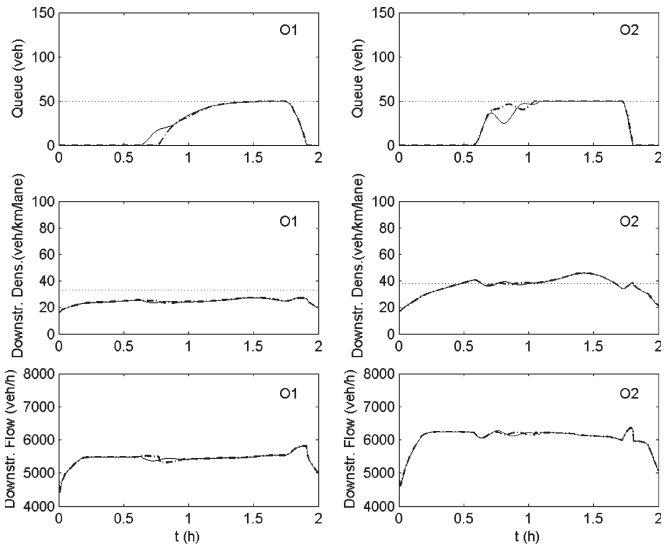

Fig. 11. Linked control on O1 and O2 with admissible queues equal to 50 veh (scenario 12 with solid lines and scenario 13 with dash-dotted lines).

different values of the activation and deactivation thresholds. It was found that the activation (deactivation) thresholds within the range [5%, 50%] ([2.5%, 25%]) lead to the activation (deactivation) of the linked control displaced by at most 2 min without any significant change in control quality. In fact, the resulting TTS/TWT values are virtually equal to those obtained for scenario 12, whereas the related ramp-queue, density, and flow profiles are very close to those already presented for the same scenario. For the activation (deactivation) thresholds that are much higher than the ones already presented, e.g., 80% (40%) (scenario 13), the linked control is activated 8 min later and deactivated just 30 s earlier. However, the minimum queue $w_{\min,o}$ ordered at the O1 is now higher during the very first control steps, and, as shown in Fig. 11 (dash-dotted lines), the queue at the O1 on-ramp is increasing faster. The resulting TTS/TWT values are once more equal to those obtained for scenario 12. These results demonstrate that the sensitivity of the proposed linked ramp-metering strategy with respect to the utilized threshold values is negligible.

In the following scenarios (14–16), the queue-control policy is active with maximum admissible ramp queue equal to 70 veh for the O1 on-ramp and 30 veh for the O2 on-ramp. In scenario 14, ALINEA is applied to both on-ramps without any coordination. Although the total storage capacity is the same as in the previous scenarios, the achieved efficiency is now reduced compared with the one achieved in scenario 10 (see Table I) as the queue at O2 reaches its maximum admissible value earlier. In contrast, the optimum open-loop solution achieved by AMOC in scenario 15 is equally efficient with the one achieved in scenario 11, as AMOC is able to efficiently exploit the available ramp storage, even if its distribution among the ramps is different. In scenario 16, the linked control is applied with an activation threshold equal to 30% and a deactivation threshold equal to 15%. Although the achieved efficiency is slightly reduced compared with the one achieved in scenario 12, the linked control still outperforms the uncoordinated local ramp metering and approximates the efficiency of AMOC.

In order to test the performance of the proposed linked-control strategy with different demand and exit-rate profiles, four additional scenarios are presented in Table II. The considered oscillatory and quite noisy profiles are shown in Fig. 12. When the no-control measures are applied (scenario 17), the resulting density and flow profiles for both merge areas are shown in Fig. 13. The mainstream congestion appears after 20 min in the merge area of the O2 on-ramp due to the high flows that arrive there; this leads to a visible gradual mainstream-flow decrease (capacity drop) that essentially persists until the end of the simulation horizon. The created congestion propagates upstream and reaches the merge area of the O1 on-ramp where the congestion has already formed. Small queues are observed at the O2 on-ramp because of the congestion in the merge area that blocks the ramp. The resulting TTS is equal to 949 veh · h and was calculated over the 2 h of simulation shown in the figures plus a cool-down period of 5 min with zero inflows. As the traffic conditions in all investigated scenarios of Table II are virtually identical over the first 20 min of the simulation (warm-up period before congestion creation), the TTS is also calculated, excluding the

TABLE II
SCENARIOS STUDIED AND RESULTS ACHIEVED FOR THE DEMAND PROFILES SPECIFIED IN FIG. 12

scenario	strategy on O1	meas. point	max queue at O1 (veh)	strategy on O2	meas. point	max queue at O2 (veh)	TWT (veh·h)	TTS (veh·h)	TTS'' (veh·h)	% decr. on TTS''
17	no-control	-	-	no-control	-	-	2	949	841	0.0
18	ALINEA	O1	70	ALINEA	O2	30	45	884	776	7.7
19	AMOC	-	70	AMOC	-	30	66	826	718	14.6
20	LC	O1	70	LC(30%-15%)	O2	30	78	853	745	11.4

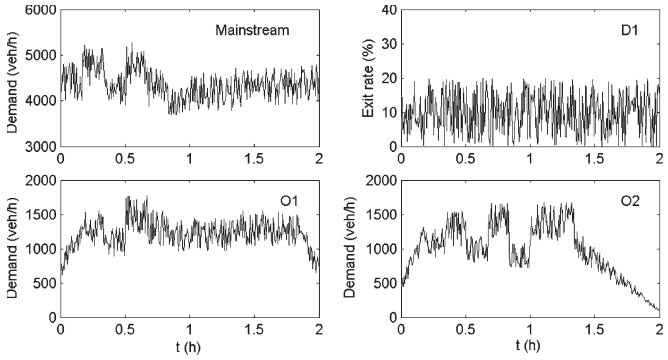

Fig. 12. Demand and exit-rate profiles used for scenarios 17–20.

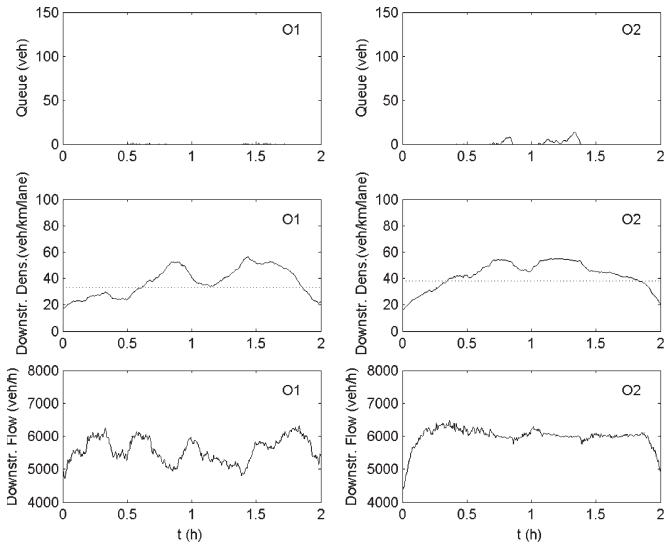

Fig. 13. No-control case (scenario 17).

first 20 min of the simulation (TTS″). The TTS″ is equal to 841 veh · h, whereas the TWT is equal to just 2 veh · h.

In the following scenarios (18–20), the queue-control policy is active with maximum admissible ramp queue equal to 70 veh for the O1 on-ramp and 30 veh for the O2 on-ramp. In scenario 18, ALINEA is applied to both O1 and O2 without coordination. The related ramp-queue, density, and flow profiles for both merge areas are shown in Fig. 14. After some 20 min of ALINEA operation, the queue at O2 reaches its maximum admissible value at around $t = 40$ min, beyond which, the queue-control regulator (3) is activated; as a consequence, freeway congestion is created that travels upstream and activates ALINEA at O1 leading to a queue for about 10 min. After $t = 1$ h, the situation in the merge area of O1 is undercritical; hence, no ALINEA activation is observed there. The TTS″ is equal to 776 veh · h, which is a 7.7% improvement compared with the no-control case, whereas the TWT is equal to 45 veh · h.

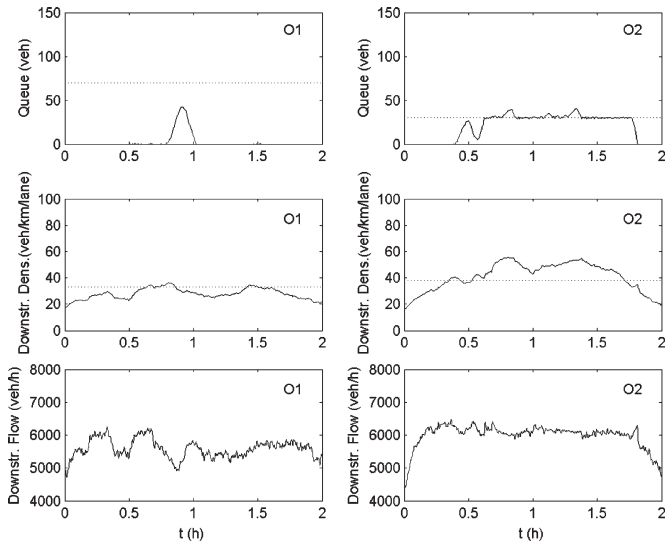

Fig. 14. ALINEA at O1 and O2 with admissible queues equal to 70 and 30 veh, respectively (scenario 18).

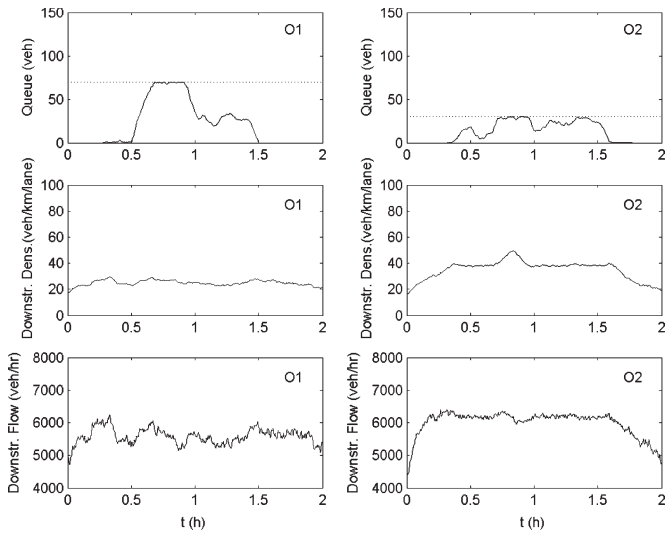

Fig. 15. Optimal open-loop solution (AMOC) with admissible queues equal to 70 and 30 veh, respectively (scenario 19).

The optimal open-loop solution obtained by AMOC in scenario 19 serves again as an "upper bound" for the achievable efficiency. The resulting TTS″ is equal to 718 veh · h, which is a 14.6% improvement compared with the no-control case, whereas the TWT is equal to 66 veh · h. The related ramp-queue, density, and flow profiles for both merge areas are shown in Fig. 15. AMOC is seen to fully exploit the available storage

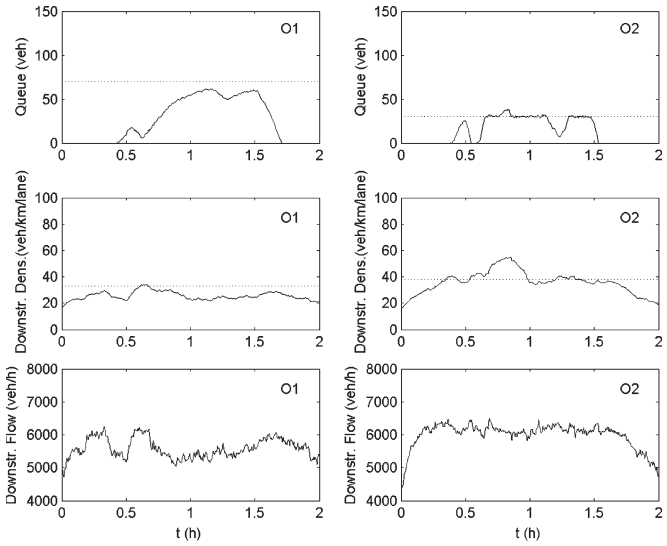

Fig. 16. Linked control on O1 and O2 with admissible queues equal to 70 and 30 veh, respectively (scenario 20).

space by simultaneously maintaining both ramps full. The mainstream outflow is maximized by maintaining the density of the O2 merge area at its critical value, except for a short period of time shortly before $t = 1$ h, where an unavoidable (due to full ramps) small congestion is seen to form.

In scenario 20, the linked control is applied with an activation threshold equal to 30% and a deactivation threshold equal to 15%. Once more, the linked control outperforms the uncoordinated local ramp metering and approximates the efficiency of AMOC. The resulting TTS$''$ is equal to 745 veh $\cdot$ h, which is an 11.4% improvement compared with the no-control case, whereas the TWT is equal to 78 veh $\cdot$ h. The related ramp-queue, density, and flow profiles for both merge areas are shown in Fig. 16. It may be seen that the storage space of the O1 ramp is exploited early in time to minimize the duration of the small congestion in the merge area of O2. This time, the linked control does not fully fill the upstream ramp, which is mainly due to the selected relatively low value of the control parameter K_{w} in (5).

VII. Conclusion

This paper has presented the results of applying the uncoordinated ALINEA, its PI extension, the AMOC optimal control, and a new linked-control strategy for the regulation of the inflow from two consecutive on-ramps to the mainstream of a long three-lane freeway axis. The obtained results lead to the following conclusions.

1) Ramp metering is a potentially valuable and efficient control measure if properly understood and applied. Some of the related subtleties and misapplications were illustrated in this paper.
2) Without the ramp-queue storage limitation, local ramp metering is highly efficient but strongly unfair (scenario 2). The limited ramp queues and the requirement of equity are the main reasons for ramp-metering coordination.
3) It makes little sense to apply local ramp metering to ramps where the mainstream congestion is imported from downstream (scenarios 4 and 5). Note that this low-efficiency behavior is currently observed in most local ramp-metering installations. What is needed in this case is a downstream bottleneck control via PI-ALINEA (scenarios 8 and 9) or a linked control.
4) Appropriately designed, the purely reactive linked control outperforms the uncoordinated local ramp metering and approximates the efficiency of the sophisticated optimal control schemes without the need for real-time modeling calculations or external disturbance prediction.

References

[1] D. P. Masher, D. W. Ross, P. J. Wong, P. L. Tuan, P. L. Zeidler, and S. Peracek, "Guidelines for design and operating of ramp control systems," Stanford Res. Inst., Menlo Park, CA, Tech. Rep. NCHRP 3–22, 1975. SRI Project 3340.

[2] M. Papageorgiou, H. Haj-Salem, and J. M. Blosseville, "ALINEA: A local feedback control law for on-ramp metering," *Transp. Res. Rec.*, no. 1320, pp. 58–64, 1991.

[3] M. Papageorgiou, H. Haj-Salem, and F. Middelham, "ALINEA local ramp metering: Summary of field results," *Transp. Res. Rec.*, no. 1603, pp. 90–98, 1998.

[4] E. Smaragdis and M. Papageorgiou, "A series of new local ramp metering strategies," *Transp. Res. Rec.*, no. 1856, pp. 74–86, 2003.

[5] E. Smaragdis, M. Papageorgiou, and E. Kosmatopoulos, "A flow-maximizing adaptive local ramp metering strategy," *Transp. Res. Part B*, vol. 38, no. 3, pp. 251–270, Mar. 2004.

[6] M. Lorenz and L. Elefteriadou, "Defining highway capacity as a function of the breakdown probability," *Transp. Res. Rec.*, no. 1776, pp. 43–51, 2001.

[7] M. J. Cassidy and J. Rudjanakanoknad, "Increasing the capacity of an isolated merge by metering its on-ramp," *Transp. Res. Part B*, vol. 39, no. 10, pp. 896–913, Dec. 2005.

[8] K. G. Keen, M. J. Schoffield, and G. C. Hay, "Ramp metering access control on M6 motorway," in *Proc. 2nd IEE Int. Conf. Road Traffic Control*, London, U.K., 1986, pp. 39–42.

[9] M. Papageorgiou, E. Kosmatopoulos, M. Protopapas, and I. Papamichail, "Evaluation of the effects of variable speed limits on motorway traffic using M42 traffic data," Dyn. Syst. Simul. Lab., Tech. Univ. Crete, Chania, Greece, Internal Rep. 2006–25, 2006.

[10] C. Diakaki and M. Papageorgiou, "Design and simulation test of coordinated ramp metering control (METALINE) for A10-West in Amsterdam," Dyn. Syst. Simul. Lab., Tech. Univ. Crete, Chania, Greece, Internal Rep. 1994–2, 1994.

[11] M. Papageorgiou, J. M. Blosseville, and H. Haj-Salem, "Modelling and real-time control of traffic flow on the southern part of Boulevard Périphérique in Paris—Part II: Coordinated on-ramp metering," *Transp. Res. Part A*, vol. 24, no. 5, pp. 361–370, Sep. 1990.

[12] M. Papageorgiou and R. Mayr, "Optimal decomposition methods applied to motorway traffic control," *Int. J. Control*, vol. 35, no. 2, pp. 269–280, 1982.

[13] O. Chen, A. Hotz, and M. Ben-Akiva, "Development and evaluation of a dynamic metering control model," in *Proc. 8th IFAC/IFIP/IFORS Symp. Transp. Syst.*, Chania, Greece, 1997, pp. 1162–1168. Preprints.

[14] H. M. Zhang and W. W. Recker, "On optimal freeway ramp control policies for congested traffic corridors," *Transp. Res. Part B*, vol. 33, no. 6, pp. 417–436, Aug. 1999.

[15] A. Kotsialos, M. Papageorgiou, M. Mangeas, and H. Haj-Salem, "Coordinated and integrated control of motorway networks via nonlinear optimal control," *Transp. Res. Part C*, vol. 10, no. 1, pp. 65–84, Feb. 2002.

[16] A. Kotsialos and M. Papageorgiou, "Efficiency and equity properties of freeway network-wide ramp metering with AMOC," *Transp. Res. Part C*, vol. 12, no. 6, pp. 401–420, Dec. 2004.

[17] G. Gomes and R. Horowitz, "Optimal freeway ramp metering using the asymmetric cell transmission model," *Transp. Res. Part C*, vol. 14, no. 4, pp. 244–262, Aug. 2006.

[18] K. Bogenberger and A. D. May, "Advanced coordinated traffic responsive ramp metering strategies," *California PATH Working Paper, UCB-ITS-PWP-99-1*, 1999, Berkeley, CA: Inst. Transp. Stud., Univ. Calif.

[19] M. A. Hadi, "Coordinated traffic responsive ramp metering strategies—An assessment based on previous studies," in *Proc. ITS World Congr.*, San Francisco, CA, 2005.
[20] I. Papamichail and M. Papageorgiou, *Traffic-Responsive Coordinated Ramp Metering for Freeway Networks*. Submitted for publication.
[21] A. Messmer and M. Papageorgiou, "METANET: A macroscopic simulation program for motorway networks," *Traffic Eng. Control*, vol. 31, no. 8/9, pp. 466–470, 1990.
[22] M. Papageorgiou, J. M. Blosseville, and H. Haj-Salem, "Modelling and real-time control of traffic flow on the southern part of Boulevard Périphérique in Paris—Part I: Modeling," *Transp. Res. Part A*, vol. 24, no. 5, pp. 345–359, Sep. 1990.
[23] A. Kotsialos, M. Papageorgiou, C. Diakaki, Y. Pavlis, and F. Middelham, "Traffic flow modeling of large-scale motorway networks using the macroscopic modeling tool METANET," *IEEE Trans. Intell. Transp. Syst.*, vol. 3, no. 4, pp. 282–292, Dec. 2002.
[24] Y. Wang and M. Papageorgiou, "Local ramp metering in the case of distant downstream bottlenecks," in *Proc. IEEE Intell. Transp. Syst. Conf.*, Toronto, ON, Canada, 2006, pp. 426–431.

Ioannis Papamichail was born in Toronto, ON, Canada, in 1976. He received the Dipl.-Eng. (honors) degree in chemical engineering from the National Technical University of Athens, Athens, Greece, in 1998 and the M.Sc. degree in process systems engineering (with distinction) and the Ph.D. degree in chemical engineering from the Imperial College London, London, U.K., in 1999 and 2002, respectively.

From 1999 to 2002, he was a Research and Teaching Assistant with the Centre for Process Systems Engineering, Imperial College London. From 2003 to 2004, he served his military service in Greece as a Chemical Engineer. From 2004 to 2005, he was an Adjunct Lecturer, and since 2005, he has been a Lecturer with the Dynamic Systems and Simulation Laboratory, Department of Production Engineering and Management, Technical University of Crete, Chania, Greece. He is the author or coauthor of several technical papers in scientific journals and conferences. His main research interests include automatic control and optimization theory and applications to traffic and transportation systems.

Dr. Papamichail is a member of the Technical Chamber of Greece. He was the recipient of the Eugenidi Foundation Scholarship for postgraduate studies from 1998 to 1999.

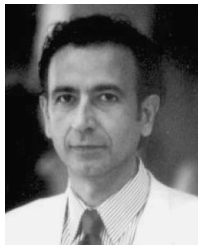

Markos Papageorgiou (M'82–SM'90–F'99) was born in Thessaloniki, Greece, in 1953. He received the Diplom-Ingenieur and Doktor-Ingenieur (honors) degrees in electrical engineering from the Technical University of Munich, Munich, Germany, in 1976 and 1981, respectively.

From 1976 to 1982, he was a Research and Teaching Assistant with the Control Engineering Chair, Technical University of Munich. He was a Free Associate with the Dorsch Consult, Munich, from 1982 to 1988 and with the Institute National de Recherche sur les Transports et leur Sécurité (INRETS), Arcueil, France, from 1986 to 1988. From 1988 to 1994, he was a Professor of automation with the Technical University of Munich. Since 1994, he has been a Professor with the Dynamic Systems and Simulation Laboratory, Department of Production Engineering and Management, Technical University of Crete, Chania, Greece. He was a Scientific Advisor of INRETS from 1988 to 1997. He was a Visiting Professor at the Politecnico di Milano, Milano, Italy, in 1982, at the Ecole Nationale des Ponts et Chaussées, Paris, France, from 1985 to 1987, and at the Massachusetts Institute of Technology, Cambridge, in 1997 and 2000. He was a Visiting Scholar at the University of Minnesota, Minneapolis, in 1991 and 1993, at the University of Southern California, Los Angeles, in 1993, and at the University of California, Berkeley, in 1993, 1997, and 2001. He is the author of the books *Applications of Automatic Control Concepts to Traffic Flow Modeling and Control* (Springer, 1983) and *Optimierung* (Oldenbourg, 1991; 1996), the coauthor of the book *Optimal Real-time Control of Sewer Networks* (Springer, 2005), the Editor of the *Concise Encyclopedia of Traffic and Transportation Systems* (Pergamon, 1991), and the author or coauthor of some 300 technical papers. His research interests include automatic control and optimization theory and applications to traffic and transportation systems, water systems, etc.

Dr. Papageorgiou is the Editor-in-Chief of *Transportation Research—Part C* and an Associate Editor of the IEEE Control Systems Society—Conference Editorial Board. He also served as an Associate Editor of the IEEE TRANSACTIONS ON INTELLIGENT TRANSPORTATION SYSTEMS. He was the recipient of the German Academic Exchange Service Scholarship from 1971 to 1976, the 1983 Eugen–Hartmann Award from the Union of German Engineers, and the Fulbright Lecturing/Research Award in 1997.